

LEGIBILITY NOTICE

A major purpose of the Technical Information Center is to provide the broadest dissemination possible of information contained in DOE's Research and Development Reports to business, industry, the academic community, and federal, state and local governments.

Although a small portion of this report is not reproducible, it is being made available to expedite the availability of information on the research discussed herein.

RECEIVED BY USN JUL 05 1985
MASTER CONF-850542--5

Los Alamos National Laboratory is operated by the University of California for the United States Department of Energy, under contract W-7405-ENG-24

**TITLE EFFECT OF POLYMER MORPHOLOGY ON PROTON AND WATER TRANSPORT THROUGH
 IONOMERIC POLYMERS**

LA-UR--85-2212

AUTHOR(S) Janine L. Fales, E-11

DE85 014086

Thomas L. Springer, E-11

Nicholas L. Vanderborgh, E-11

Pieter Stroeve, University of California, Davis

SUBMITTED TO

Proceedings volume of the Engineering of Industrial Electrolytic
 Processes Symposium of the Industrial Electrolytic Division held at
 the Electrochemical Society Meeting, Toronto, Canada, May 12-17, 1985

DISCLAIMER

This report was prepared as an account of work sponsored by an agency of the United States Government. Neither the United States Government nor any agency thereof, nor any of their employees, makes any warranty, express or implied, or assumes any legal liability or responsibility for the accuracy, completeness, or usefulness of any information, apparatus, product, or process disclosed, or represents that its use would not infringe privately owned rights. Reference herein to any specific commercial product, process, or service by trade name, trademark, manufacturer, or otherwise does not necessarily constitute or imply its endorsement, recommendation, or favoring by the United States Government or any agency thereof. The views and opinions of authors expressed herein do not necessarily state or reflect those of the United States Government or any agency thereof.

By acceptance of this article the publisher recognizes that the U.S. Government retains a nonexclusive, royalty-free license to publish or reproduce the published form of this contribution or to allow others to do so for U.S. Government purposes.

The Los Alamos National Laboratory requests that the publisher identify this article as work performed under the auspices of the U.S. Department of Energy.

DISTRIBUTION OF THIS DOCUMENT IS UNLIMITED

Los Alamos Los Alamos National Laboratory
 Los Alamos, New Mexico 87545

**EFFECT OF POLYMER MORPHOLOGY ON PROTON AND WATER TRANSPORT
THROUGH IONOMERIC POLYMERS**

by

Janine L. Fales^{1,2}, Thomas E. Springer¹ and Nicholas E. Vanderborgh¹

¹Electronics Division
Los Alamos National Laboratory
Los Alamos, NM 87545

and

Pieter Stroeve²

²Department of Chemical Engineering
The University of California
Davis, CA 95616

ABSTRACT

The rate of ionic transport through perfluorosulfonic acid membranes is set by water content within mass transfer channels of the polymer. Consequently, control of water flux is important to control transport rates. Experiments show the influence of cation type on water transport properties and on polymer physical properties. These results support the model that channel geometries are determined by the interaction of coulombic forces within the membrane. Description of these transport processes is accomplished through several mathematical routes.

INTRODUCTION

Ion exchange membranes serve well as cell separators in electrochemical systems used for energy conversion (fuel cells) (1,2) or chemical synthesis (especially water electrolysis) (3). In these systems, the membrane separates the anode from the cathode while maintaining high, selective ionic conductivity. Efficiency of these devices demands high conductivity and, at times, high ionic selectivity, where specific ionic transference numbers approach unity. During the last decade, there has been considerable progress in developing polymeric materials that are suitable for this separator task.

Although early work used sulfonated polystyrene membranes, the chemical and mechanical stability of polyperfluorosulfonic acids, such as Du Pont's Nafion class of polymers, has become increasingly attractive (4,5). These ion exchange polymers, like their predecessor ion exchange resins, imbibe considerable quantities of water. For instance, ion exchange membranes flood with water to values of 50%, or more, of the dry weight. However, these materials sustain mechanical strengths even when water-filled, demonstrating a continuous polymer phase. Therefore, structural models show two continuous phases, one with ionic properties similar to an aqueous solution, and the other with polymer properties similar to polytetrafluoroethylene.

Ionic transport is an important parameter in membrane utilization. Studies conclude that increased moisture content (weight per cent) increases ionic conductivity values. Membranes are readily expanded to imbibe additional water by increasing the pretreatment temperature. The polymer retains moisture resulting from the highest pretreatment temperature, even when used at a lower temperature. Molecular transport is also important. For instance, during hydrogen-oxygen fuel cell operation, water is a product of the cathodic reaction. Depending upon temperature and pressure, water will exhaust either as a liquid or a gas, and depending upon the differential pressure across the membrane, considerable water may flow from the cathodic to the anodic region (6). This flow is countercurrent to both the ionic or proton flux and to the water flux associated with the protons. Control of water concentration levels within the membrane requires an understanding of those polymer features that control water transport.

The details of transport dynamics in ionomers such as Nafion are complicated because the polymer morphology appears set by the ionic structures that exist within the polymer. Our work, and others, suggests that these morphological channels -- those structural features that establish flow rates -- are the result of dynamic interactions between opposing forces within the polymer. Elastic moduli forces act to structure the polymer while anionic repulsion forces tend to distend the material. The stabilizing forces are a function of temperature as established by elastic moduli terms while the anionic repulsion forces are set through a different dependence on temperature, as described by the Boltzmann distribution. Thus, in a quantitative way, the temperature influences structural parameters, such as swelling, represented by water content.

These earlier calculations also established details of cation interactions within these systems (7). In those studies, we considered the anion-cation separation dynamics within ionomers. Results, based on statistical mechanical calculations, showed that the monovalent cations are most probable at small distances from the locus of the fixed anionic charge. In fact, assuming that these anionic species set the position of a "pore wall," then cations form a double layer close to this same location. When the calculation is accomplished using point charges, most probable cation locations are within 0.5×10^{-8} cm

of the anionic wall position. Because this location is smaller than hydrated ionic diameters, finite-sized ions will assume different equilibrium distances because larger ions cannot approach the "pore wall" as easily as smaller ones. This result shows that larger cations exhibit less "screening" of the anionic charge than small cations. (Alternatively, one could discuss inner-outer sphere coordination complexes and conclude that smaller cations approach the sulfonic acid, anion groups to form a contact ion pair.) Larger cations, especially those cations that maintain a large hydrated complex, are less effective in localizing anionic charge. In that case, the anions experience maximum interanion repulsion and the polymer distends. Cations that result in contact ion pairs diminish the anion repulsion forces. Then the constant modulus terms contract the polymer to yield a decreased "water content" and a smaller molecular volume.

Most workers conclude that these polymers conform to generate clusters of ions, rather like solution micelles (1). These clusters represent both sites where high, compared to average, ionic charge occurs and, consequently, locations where significant fractions of water reside. Clusters within wet polymer samples are examined by low-angle x-ray scattering or with neutron diffraction. Clusters can also be examined in dry polymer samples with scanning electron microscopy provided cations such as Ag^+ are introduced before dehydration. Both of these spectral techniques lead to structural models that show arrays of clusters with uniform, periodic distribution.

These ordered ionic regions can result either from statistical variations caused during polymer synthesis, such as a nonrandom distribution of the side chain position on the polyfluoroethylene backbone, or from ordering on ionic sites within the previously formed solid. At present, we cannot state which effect is dominant; however, we assume that the second is most probable. In that case, we must consider polymer morphology, especially predicted conformations of the solid material. These polymers, perhaps like many biopolymers, may order into a helical conformation with anionic side chains merged to form ionic clusters. Figure 1 depicts that one cluster results from merged anionic groups on three adjacent "coils" of the helical conformation. Those on the upper turn merge with one turn below, and those on the next lower turn conform "upward" to form one cluster. Anion chain length precludes groups from decks farther away than two turns. This three-level stack then leads to a cluster of 30-50 sites, depending upon the diameter of the helix. Farther up and down the chain, other clusters form in a similar fashion. This qualitative representation explains the formation of these clusters and their three-dimensional nature, and accounts for the measured intracluster distances.

The average cluster size across the membrane may not be uniform during transport as suggested, for example, by the studies of Fabiani et al. (8,9) who experimentally measured a decrease in the characteristic pore size with ionic concentration. The screening of wall charges by hydrogen ions decreases the electrostatic repulsive forces

by the charged sulfonic acid groups and causes a partial collapse of clusters and channels. The importance of mechanochemical forces in transport in charged polymers such as collagen has been reviewed by Grodzinsky (10). Iisu and Gierke (11,12) have attempted to incorporate the variation of cluster size with water content, taking into account the elastic energy of the polymer, but the incorporation of their results into a capillary pore transport model is not obvious.

Transport through these materials occurs through channels set by dynamic charge distributions and elastic strength. This paper discusses current mathematical formulations used to predict molecular and ion transport and presents experimental results that explore the interaction of polymer morphology on these transport processes.

MATHEMATICAL PREDICTION OF TRANSPORT

Modeling the transport of hydrogen ions and water in these ionomeric membranes normally must implicitly include polymer morphology. The formation of ionic clusters within perfluorinated sulfonic acid membranes is now widely accepted, but uncertainty exists about the ionic cluster size, the interconnectivity of the clusters, the size and shape of the connecting channels, the state of water within the pores, and the manner that hydrogen ions move through the pores. It has been assumed that significant transport occurs solely in the pore structure and not in polymer-rich regions. Although most work assumes a series of regular pores, the assumptions that are made to represent membrane morphology must be kept in mind because they introduce a measure of empiricism to the theoretical results.

The simplest pore structure consists of uniform, parallel capillaries that traverse the membrane from the anode to the cathode side; this morphology, however, has only limited physical reality. When one considers the cluster-channel network concept, the first question of importance is the characteristic pore diameter. The characteristic pore diameter must accurately represent the characteristic cluster size, the channel size, and the interconnectivity of clusters including dead-end pores. At present, there is no self-consistent manner to obtain a characteristic pore size from these mass transport features.

Previous modeling of ion and water transport through ionic exchange membranes can be classified into one of three categories:

1. continuum mechanics,
2. irreversible thermodynamics (Stefan-Maxwell equations), and
3. percolation theory.

Continuum theories can be divided into continuum-mechanical and irreversible thermodynamics models. Application of the continuum-mechanical model to transport in uniform pores is documented by Westermann-Clark and Anderson (13), who concluded from experiments

that the model is quantitatively accurate for pores larger than 3.0×10^{-7} cm in radius and for aqueous electrolyte concentration of 0.1 M or lower. The success of continuum equations, such as the Nernst-Planck equation, for such small pores is surprising. A discussion of the basis and limitations of the Nernst-Planck equation in ionic transport has been given by Buck (14). He argues that, when pores and channels become on the same size order as molecules, this mathematical approach is not correct. Nevertheless, Koh and Silverman (15) have applied the continuum-mechanical model to transport of hydroxyl ions in Nafion membranes and have obtained intuitively consistent results. Their results showed that the ionic fluxes are controlled by pore dimensions and pore surface charge densities. It is not known if their results are fortuitous or if the continuum-mechanical model can be consistently applied with success to model transport in Nafion membranes where pore sizes are on the order of 1.0 to 4.0×10^{-7} cm. In addition to the noncontinuum criticism, the continuum-mechanical model is not easy to apply to complex pore structures due to uncertainties in formulation of wall boundary conditions. This problem might be circumvented in part by using finite element or boundary element techniques.

Irreversible thermodynamics, in the form of the closely related Stefan-Maxwell equations, have been used by Pintauro and Bennion (16,17) to obtain transport coefficients from experimental data on dialysis, electrodialysis, and reverse osmosis for NaCl and water transport across Nafion membranes. Unlike the continuum-mechanical model, irreversible thermodynamics is a continuum approach that does not consider microscopic information about pore morphology. As in the continuum-mechanical approach, the consistency of a given pore model can be checked with experimental data to give one or more characteristic empirical parameters that describe morphology.

Percolation theory has been applied by Hsu et al. (11,18) to model the threshold value of the aqueous volume fraction for which the polymer first becomes proton conductive. In this approach, the state of interdispersion of materials in a heterogeneous medium is randomly stated. For Nafion, binary interdispersion is used to represent void (or cluster) and purely polymer space. The method of generating a heterogeneous medium depends on the choice of tessellation, which is the juxtaposition of similar elements of either void or polymer phase in a coherent pattern. Hsu and Gierke (11) have used cubic tessellation, but there are other possible choices, such as lamellar or polyhedron (Voronoi) structures. Consequently, the choice of tessellation involves an empiricism similar to selecting a pore model using the continuum-mechanical approach.

The percolation method has not been fully developed to obtain other transport parameters, especially the hydraulic permeability and pore electrical conductivity. Similar to the characteristic pore size varying from one side to the other side of the membrane, the cluster volume fraction can also vary across the membrane if a sufficiently large gradient exists.

Although each of these approaches has been used extensively, a credible explanation of transport through these systems is lacking. The central problem in applying transport models to Nafion membranes is the question of the morphology of the polymer and the interactive role water and hydrogen ions play in determining morphology. In order to include these variations of morphology, we have approached the problem by using molecular dynamics to establish the three-dimensional channel morphology. Once the morphology is established, continuum models can be used to predict transport properties.

Whereas molecular dynamics have never before been applied to Nafion (to our knowledge), the method has been used extensively in the biochemical field to predict transport in biological membranes. Fraga and Milar (19) have used molecular dynamics to theoretically simulate ionic transport through gramicidin A, which has naturally occurring charged, transmembrane channels. By using molecular dynamics, we are able to take into account the size of the water molecules, the sulfonic acid side groups, and the ions within the Nafion channel. The basic method is to let a representative number of molecules and ions move according to the forces (electrostatic and van der Waals) operating on them. In our calculations, soft potentials and periodic boundary conditions are used. Table 1 summarizes the models and the advantages of each.

EXPERIMENTAL

Nafion 117 supplied by E. I. Du Pont de Nemours & Company, Incorporated, is an unreinforced perfluorinated sulfonic acid ionomer, with an equivalent weight (EW) of approximately 1100 and a dry thickness of 0.018 cm. The membrane specimens were treated before use by boiling the hydrogen form in deionized water for 4 hours under 20 psig (109°C).

Measurements of membrane properties, such as thickness, weight, and water content, were taken under equilibrium conditions. Exchange of other ions was accomplished by soaking a pretreated membrane in a 1.0 M solution for 24 hours at a constant temperature. Membranes were then rinsed by sonicating them in water for 2 hours, with a change in water every 15 minutes. Solutions of HCl, LiCl, NaCl, KCl, and CsCl were used at 25°C.

Thicknesses were measured with a digital thickness gauge and with a micrometer. After the 24-hour equilibration period, the membrane sample was removed from solution and excess solution was blotted from the surface with filter paper. The thickness was then measured in at least three locations with both devices. After completing the thickness measurement, we promptly weighed the membrane sample and measured the dimensions. The sample was then placed in a desiccator to dry at 25°C, until its weight became constant. The difference in wet and dry weights represented the membrane water content.

Water removal from Nafion polymers permits an evaluation of molecular transport in the absence of auxiliary electrolyte solutions. A series of experiments was accomplished where a water-filled polymer sample was dried in a flowing gas stream while the sample mass was monitored. These experiments were accomplished using a custom sample holder that suspended the polymer within the sample chamber of a Mettler TG-50 thermobalance. Here, the polymer studied was in the proton form. Dry argon gas (trapped to a water content of less than 1 ppm) was used for drying.

A pressure-flow apparatus was constructed to measure the effective porosity of Nafion membranes as a function of ionic form and temperature. This was done by monitoring the pressure drop across a specimen under conditions of constant water flow and temperature. Figure 2 shows a schematic diagram of the system. A high-pressure, low-flow, precision-metering pump was used to set a continuous flow, and then pressure on each side of the sample was monitored. The sample was held in a stainless steel, high-pressure flange, and the temperature within the heated chamber was regulated to $\pm 0.4^\circ\text{C}$. The back pressure was maintained at 52 ± 0.2 psi. The experiment proceeded until a steady-state value for the pressure drop was achieved for a given flow rate.

Polymer physical strengths were measured by monitoring the extension caused by known force loads, while the material was submerged under a specified test solution and maintained at a fixed temperature. This apparatus (see Fig. 3) was constructed using reinforced fiber glass to minimize the effects of foreign ions that might be released from ferrous materials. Wet Nafion strips were mounted and allowed to dry in the absence of force. Length was recorded. The experiment was then repeated after suspending an 800 g weight, which established a constant force, and the length was again recorded. The sample was submerged in 1 M CsCl solution. Length was recorded as a function of time until no further length change was detected. The sample was removed from the solution, rinsed with deionized water, and allowed to dry without the applied force. This procedure was repeated with the same Nafion sample for solutions of 1 M KCl, NaCl, LiCl, and HCl, in that order. Temperature was maintained to $\pm 0.1^\circ\text{C}$ with a circulating water bath.

RESULTS AND DISCUSSION

Experiments were conducted to deduce molecular flow features through Nafion 117 samples. Of particular interest are those measurements that reflect channel dimensions because those values are necessary input for molecular dynamic calculations. Equilibrium water concentration results are given in Table 2, which shows properties of wet membranes as a function of cation. For comparison, water contents of Nafion 125 [as reported by Hsu and Gierke (11)] and properties of the dry polymer are included. These data show the well-known trend of wide variations in water content as the nature of the cation is changed.

Increased water content of the lower equivalent weight polymer (117) compared with the 125 material is expected because of the increased number of sulfonic acid side chains in the 117 material.

Data were determined for exploring the dehydration of Nafion 117, especially searching regions of the drying curve that represent stable, hydrate regimes. Water loss began immediately at room temperature and continued until about 50°C, when the rate decreased. Between 50 and 180°C, mass losses continue but at a slower rate. Finally, a steady weight is obtained between 180 and 350°C. At higher temperatures, the polymer began to decompose, although there was no evidence of charring or loss of physical strength; rather, the material mass continuously decreased, perhaps through an unzipping mechanism. If one assumes that the polymer mass at 180°C is the "dry" weight and if one knows the equivalent weight, the number of water molecules per sulfonic acid group can be calculated. (This method of determining water content gives approximately the same results, within 5%, as the equilibrium water values mentioned above because most (90%) of the water exhausts rapidly at relatively low temperatures.) In these equilibrium studies with Nafion 117, the wet polymer reaches a condition, near 50°C, where three water molecules remain per site. At 100°C, a single water molecule, on the average, is associated with each site, perhaps because of a close contact pair, $R-SO_3H_3O^+$. Then, at higher temperatures, this compound decomposed. There is no evidence of other specific molecular hydrates, rather these data show a continuous water flow from the sample with the highest rates in the region of 25-50°C.

Water loss kinetics can be described by one of two models, essentially limited by the rate of heat transfer to the evaporation surface or by the rate of mass transfer to that surface. The initial rate of water loss was determined at each of three temperatures, 25, 30, and 35°C. Water loss rates increased as temperatures were increased, but the data suggest that the loss was controlled by mass transport. Individual samples were rectangular, and within 1-2%, the surface area is given by

$$A_t = 2m/dl \quad ,$$

where

- A_t = surface area in cm^2 of the two sample sides,
- m = dry polymer mass,
- l = polymer thickness, and
- d = dry polymer density.

The water loss rate was taken as the slope of the weight vs. time curve. Results are given in Table 3.

These results show that the product of the initial drying rate, multiplied by the water viscosity, normalized for surface area, is a constant, k' . Water transport in this case appears controlled by the

rate of flow through the microporous polymer. These results parallel those that have shown water permeability rates solely influenced by fluid dynamic parameters (viscosity) as long as ionic forces within the polymer are set (same pretreatment temperature and cation type).

The rate of water transport through the polymer, then, is controlled by the morphology of the microporosity. This structural set can be varied by altering the ionic-charge distributions within the material. This alteration is readily accomplished by changing the cation type. One way of describing these changes is to measure an effective channel diameter by determining the fluid dynamics through a polymer sheet. We chose to determine an effective pore radius, r_{eff} , using the Hagen-Poiseuille equation for laminar flow (20):

$$r_{eff}^4 = 8 \mu l Q / (\Delta P \pi)$$

where

μ = viscosity,
 l = thickness,
 Q = flow rate,
 ΔP = pressure drop, and
 r_{eff} = effective pore radius.

This equation calculates the effective radius of a single channel that will sustain the measured flows. For a distributed porosity, such as we are considering here, the average pore diameter could be estimated by dividing this value by the number of pores. As indicated in Fig. 4, these results show that channel diameters are directly related to the size of the monovalent hydrated cations. The largest hydrated ions distend the polymer the most to give the largest effective pore radii. This linear relationship between cation size and molecular flow suggests that molecular parameters are set by the double layer structure. Statistical mechanics results show that charges are concentrated at channel walls, and thus, we conclude that the channel geometry results from electrostatic forces. Larger cations do not approach the channel "wall" to the same extent as the smaller cations. Protons, especially the large hydrated ions in these polymer systems, are less effective at decreasing interanionic repulsive forces because they do not approach the wall potential to the same extent as smaller univalent cations. These results are in general agreement with those given by dynamic calculations of charge distributions within polymer channels.

The physical strength of a polymer is intimately related to the forces acting within the polymer. These ionomeric polymers are physically strong, rather like PTFE materials. This morphological model is based on the alteration of ionic forces effected by changing the size of the hydrated cations. Elastic moduli forces should reflect these alterations for the polymer intermolecular forces need to both sustain material strength and to counteract the swelling forces, driven by the ionic dynamics. Therefore this model predicts that the polymer will lose strength as the channel dimensions increase.

A novel series of experiments was accomplished to explore the distention of the polymer as a function of cation type and of temperature. These results are given in Fig. 5. Although quantitative conclusions on actual forces within the polymer cannot be deduced from these data, results again support the general concept above. The polymer in its distended hydrogen form is considerably weaker than when swelling is decreased. The differences in strength appear because of the effectiveness in anionic repulsion screening since the forces caused by the elastic moduli of the polymer are set with temperature.

CONCLUSIONS

These results illustrate the sharp alteration of molecular transport through these ionomer sheets that are caused by variation of ionic distributions within the cluster sets. Because ionic distributions must vary during dynamic ionic transport, we expect that useful models of transport will incorporate specified channel dimensions as a function of operating conditions.

These results corroborate those concepts suggesting that morphological channels controlling transport properties result from the interaction of polymer moduli forces and ionic repulsion forces. Normally, these two forces sum to form a state of tension within these materials that establishes transport features. Molecular transport varies directly with the hydrated cation size. It appears that moisture floods into the interior of these materials until the available porosity is water filled. Thermobalance data show that water exhausts, even at room temperature, at rates set by the channel size. At higher temperatures, water concentrations result from a sum of localized generation and discharge rates. Thus, although water content is a function of swelling, ionic forces set the swelling extent, not the moisture content. Water content is a dynamic parameter set by fluid dynamic rates.

Models that explain transport through these materials should include the effects of channel feature variations on the mass transport process. This now appears feasible because molecular dynamics models, based on sensible assumptions of channel geometries, can serve as the base for establishing channel dimensions. Once these are known in a spatially dependent way, set by the current and transport rates, then existing formulations of continuum mechanics will give a dynamic picture of transport through these polymers. Work on this subject will be the topic of future papers.

ACKNOWLEDGEMENTS

The authors thank Mr. Amitav Hajundar for his valuable input into the experimental design, his assistance in carrying out experiments, and his stimulating conversations throughout this work. They also appreciate the expertise of Mr. Michael Haertling, Mr. Chuck Derouin, and Mr. Fred Kelley in the construction of special apparatus used. The authors acknowledge the support of this work by the United States Department of Energy.

REFERENCES

1. Adi Eisenberg and Howard L. Yeager, Editors, Perfluorinated Ionomer Membranes, ACS Symposium Series No. 180, Washington D.C. (1982).
2. James F. McKelroy and Lynn J. Nuttall, "Status of Solid Polymer Electrolyte Fuel Cell Technology and Potential for Transportation Applications," 17th Meeting of the IECEC, Paper Number 829371, 667 (1982).
3. Jean Sarrazin and Andre Tallec, "Use of Ion Exchange Membranes in Preparative Organic Electrochemistry: New Processes for Electrolysis," J. Electroanal. Chem. 137, 183 (1982).
4. Anon., NAFION, Perfluorosulfonic Acid Products, DuPont Company, Polymer Products Department, Wilmington, DE 19898, E-47754 (April 1982).
5. W. Grot, "Perfluorierte Ionenaustauscher-Membrane von hoher chemischer und thermischer Stabilität," Chemie-Ing.-Techn. 44, 167 (1972).
6. Nicholas E. Vanderborgh and Thomas E. Springer, "Water Flow Through Solid Polymer Electrolytes (SPE) During Fuel Cell Operation," extended abstracts of the Washington Electrochemical Society Meeting, Washington D.C., October 9-14, 1983.
7. Nicholas E. Vanderborgh and Thomas E. Springer, "Proton and Water Transport Through SPE Membranes," extended abstracts of the San Francisco Meeting of the Electrochemical Society, San Francisco, CA, May 8-13, 1983.
8. C. Fabiani, G. Scibona, and B. Scuppa, "Correlations between Electroosmotic Coefficients and Hydraulic Permeability in 'Nafion' Membranes," J. Membr. Sci. 16, 51 (1983).
9. C. Fabiani, B. Scuppa, L. Bimbi and M. DeFrancesco, "Filtration Coefficient and Hydraulic Permeability of Nafion 125 Membranes in Metal Alkali Solutions," J. Electrochem. Soc. 130, 583 (1983).

10. Solomon R. Risenberg and Alan J. Grodzinsky, "Electrically Modulated Membrane Permeability," J. Memb. Sci. 19, 173 (1984).
11. William Y. Hsu and Timothy D. Gierke, "Ion Clustering and Transport in 'Nafion' Perfluorinated Membranes," extended abstracts of the 161th Meeting of the Electrochemical Society, Montreal, May 1982.
12. William Y. Hsu and Timothy D. Gierke, "Elastic Theory for Ionic Clustering in Perfluorinated Ionomers," Macromolecules 15, 101 (1982).
13. G.B. Westermann-Clark and J. L. Anderson, "Experimental Verification of the Space Charge Model for Electrokineics in Charged Microporous Membranes," J. Electrochem. Soc. 130, 839 (1983).
14. Richard P. Buck, "Kinetics of Bulk and Interfacial Ionic Motion: Microscopic Bases and Limits for the Nerst-Planck Equation Applied to Membrane Systems," J. Memb. Sci. 17, 1 (1984).
15. W. H. Koh and H. P. Silverman, "Anion Transport in Thin-Channel Cation Exchange Membranes," J. Memb. Sci. 13, 279 (1983).
16. Peter N. Pintauro and Douglas N. Bennion, "Mass Transport of Electrolytes in Membranes: I. Development of Mathematical Transport Model," I&EC Fund. 23, 230 (1984).
17. Peter N. Pintauro and Douglas N. Bennion, "Mass Transport of Electrolytes in Membranes: II. Determination of NaCl Equilibrium and Transport Parameters for Nafion," I&EC Fund. 23, 234 (1984).
18. William Y. Hsu, John R. Barkley, and Paul Meakin, "Ion Percolation and Insulator-to-Conductor Transition in 'Nafion' Perfluoro-sulfonic Acid Membranes," Macromolecules 13, 198 (1980).
19. Serafin Fraga and S.H.M. Nilar, "Theoretical Simulation of Ionic Transport through a Transmembrane Channel," Canadian J. of Biochem. and Cell Biol. 61, 856 (1983).
20. R. Byron Bird, Warren E. Stewart, and Edwin N. Lightfoot, Transport Phenomena (John Wiley & Sons, Inc., New York, 1960), p. 46.

TABLE 1: SUMMARY OF APPROACHES FOR TRANSPORT MODELING

METHOD	ADVANTAGES
<u>Continuum Theories;</u> continuum-mechanical and irreversible thermodynamics models	Well established; ease of computation; for assumed pore geometry, transport parameters can be derived from direct experiments and compared with predictions.
<u>Percolation Theory</u>	Method for generating random heterogeneous media; predicts critical pore volume fraction for conduction to occur.
<u>Molecular Dynamics</u>	Incorporation of noncontinuum effects; incorporation of com- plex pore structures.

TABLE 2: PHYSICAL PROPERTIES OF WET POLYMER (NAFION) AT 25°C

Cation	Thickness (cm x 10 ²)	Density (g/cm ³)	w/w% H ₂ O Nafion 117	w/w% H ₂ O Nafion 125
H ⁺	2.41	1.46	45.0	33.6
Li ⁺	2.23	1.56	40.4	29.7
Na ⁺	2.16	1.76	36.6	21.0
K ⁺	2.03	2.01	25.2	8.7
Cs ⁺	1.91	2.11	18.7	5.9
H ⁺ (dry)	1.80	2.10	-	-

TABLE 3: INITIAL RATES OF WATER REMOVAL FROM NAFION 117 (IN DRY ARGON)

Temperature, °C	25.0	30.0	35.0
Water Loss Rate, mol/s x 10 ⁶	1.34	1.42	1.63
Water Viscosity, cp	0.880	0.800	0.741
Area, cm ²	4.99	4.82	4.73
k' ^a x 10 ⁷	2.4	2.4	2.6

^a k' shows the (water loss rate x area)/(viscosity) value.

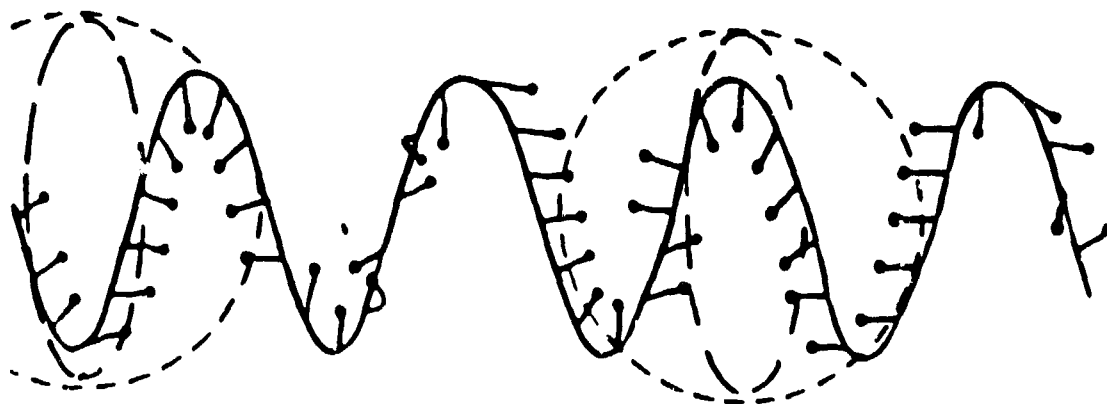


Figure 1: Helical Conformation of Perfluorosulfonic Acid Polymers. This sketch represents a helical conformation of Nafion-like polymers. Polymer chains coil, moving the pendant ionic groups to alternative clusters that focus at every third deck in the helical coil. Cations are not shown.

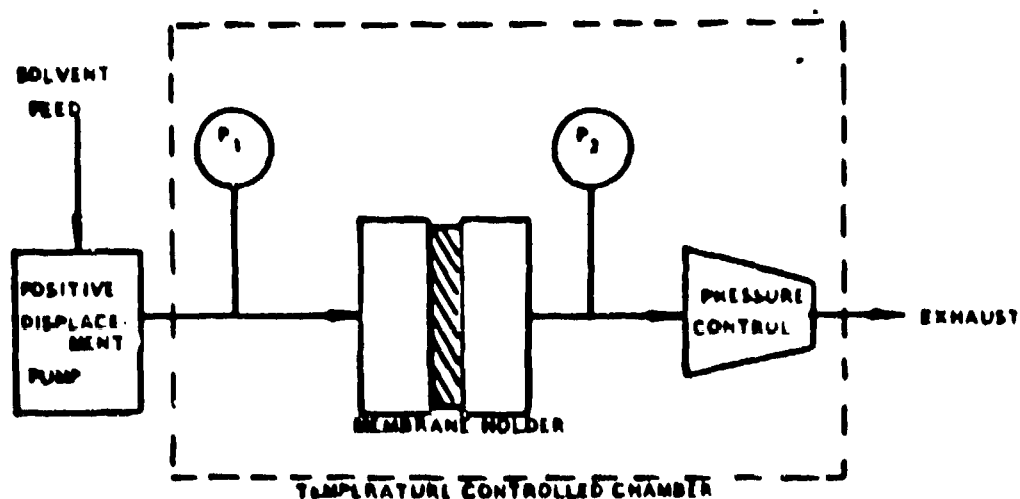


Figure 2: Pressurized Permeability Instrument: Solvent (water, etc.) is pumped with known flow rate through membrane specimen with cross sectional area, A . Upstream and downstream pressure measurements determine membrane pressure drop. Apparatus permits temperature studies between ambient and 150°C and pressures from 1 to 50 atmospheres.

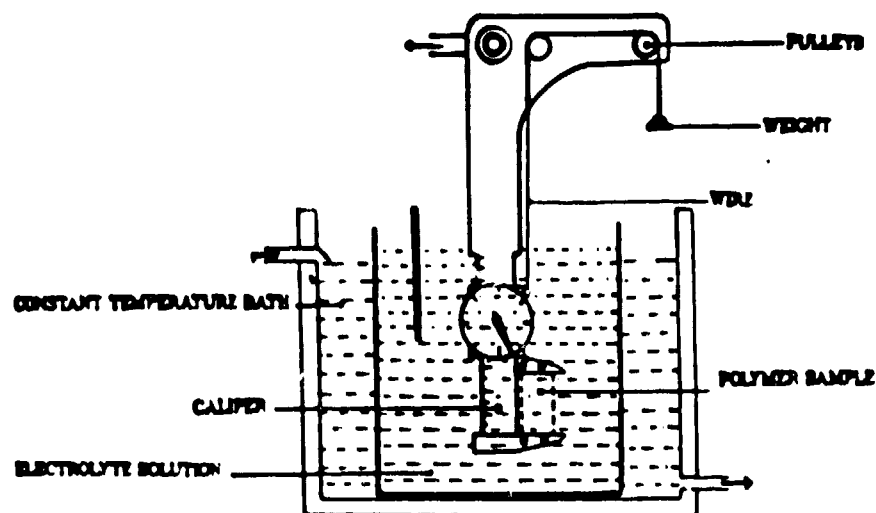


Figure 3: Polymer Elongation Instrument: Pretreated polymer sample is clamped between caliper jaws and sample size measured as fixed force is exerted by a weight (0 to 1000 g). Sample clamp is constructed from polymeric materials to minimize corrosion and ionic contamination. Control can vary from ambient to boiling point temperatures.

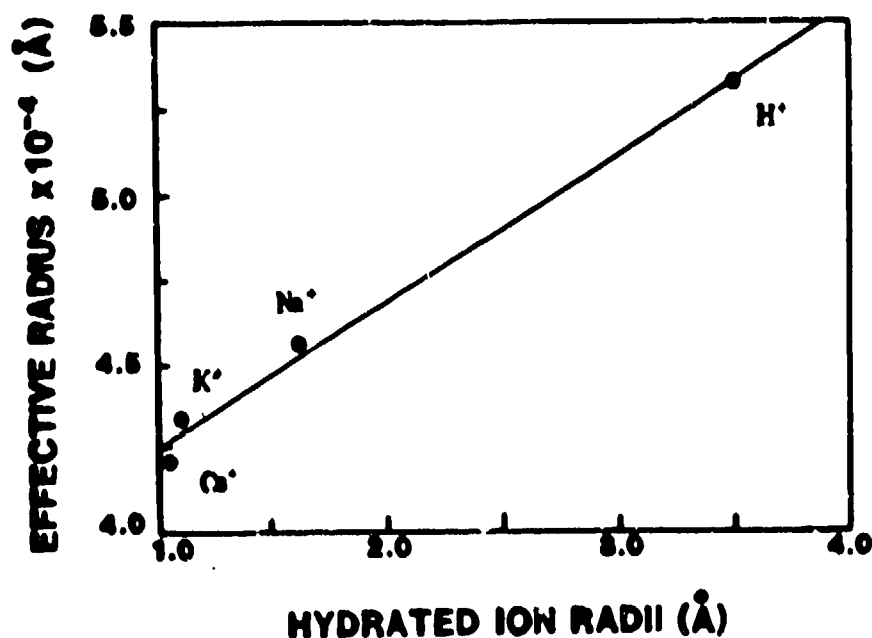


Figure 4: Effective Pore Radius Contrasted to Hydrated Cation Size. Results show calculated pore radius, the radius of a single pore that sustains measured hydraulic flow through polymer, contrasted to hydrated cation size. Actual pore geometries are determined by dividing the effective radius by the number pore density.

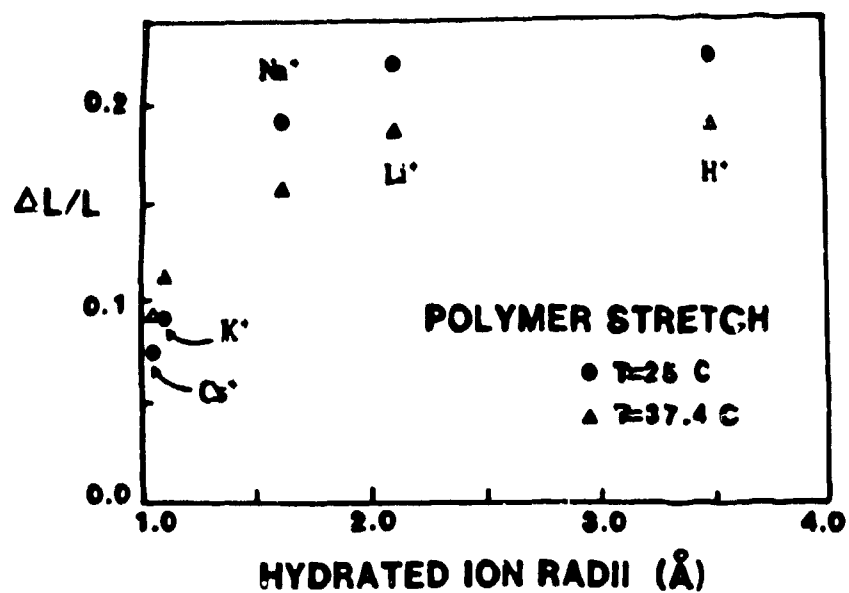


Figure 5: Polymer Elastic Modulus: Results show relative extension for a single polymer sample in each of four cationic forms and at two temperatures. Experimental procedure is described in text.